

DDColor: Towards Photo-Realistic and Semantic-Aware Image Colorization via Dual Decoders

Xiaoyang Kang, Tao Yang, Wenqi Ouyang, Peiran Ren, Lingzhi Li, Xuansong Xie
DAMO Academy, Alibaba Group

{kangxiaoyang.kxy, baiguan.yt, wenqi.oywq, peiran.rpr, llz273714, xingtong.xxs}@alibaba-inc.com

Abstract

Automatic image colorization is a particularly challenging problem. Due to the high illness of the problem and multi-modal uncertainty, directly training a deep neural network usually leads to incorrect semantic colors and low color richness. Existing transformer-based methods can deliver better results but highly depend on hand-crafted dataset-level empirical distribution priors. In this work, we propose DDColor, a new end-to-end method with dual decoders, for image colorization. More specifically, we design a multi-scale image decoder and a transformer-based color decoder. The former manages to restore the spatial resolution of the image, while the latter establishes the correlation between semantic representations and color queries via cross-attention. The two decoders incorporate to learn semantic-aware color embedding by leveraging the multi-scale visual features. With the help of these two decoders, our method succeeds in producing semantically consistent and visually plausible colorization results without any additional priors. In addition, a simple but effective colorfulness loss is introduced to further improve the color richness of generated results. Our extensive experiments demonstrate that the proposed DDColor achieves significantly superior performance to existing state-of-the-art works both quantitatively and qualitatively. Codes will be made publicly available at <https://github.com/piddnad/DDColor>.

1. Introduction

Image colorization is a classic computer vision task and has great potential in many real-world applications, such as legacy photo restoration [38], video remastering [20] and art creation [34], etc. Given a grayscale image, colorization aims to recover its two missing color channels, which is highly ill-posed and usually suffers from multi-modal uncertainty, e.g., an object may have multiple plausible colors. Traditional colorization methods address this

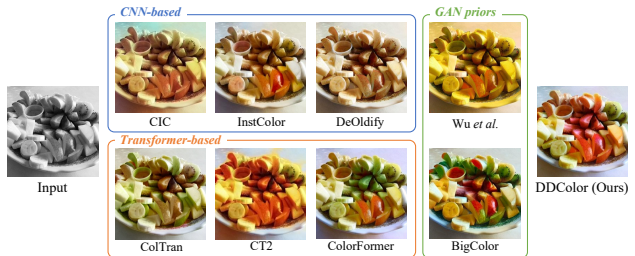


Figure 1. **Visual comparison.** *Top left:* The CNN-based methods usually yield unsaturated results. *Middle Right:* Methods based on GAN priors tend to produce inappropriate colorization or unpleasant artifacts. *Bottom left:* Transformer-based methods fail to tackle images with complex contexts, resulting in semantically incorrect or inconsistent colors. *Right:* The proposed DDColor is capable of generating realistic and diverse colorization results.

problem mainly based on user guidance such as reference images [9, 13, 21, 26, 41] and color graffiti [24, 31, 34, 46]. Although great progress has been made, it remains a challenging research problem.

With the rise of deep learning, automatic colorization has drawn a lot of attention, targeting at producing appropriate colors from complex image semantics (e.g., shape, texture, and context). Some early methods [1, 8, 10, 37, 47] attempt to predict per-pixel color distributions using convolutional neural networks (CNNs). Unfortunately, these CNN-based methods often lead to incorrect or unsaturated colorization results due to the lack of a comprehensive understanding of image semantics (Fig. 1 CIC [47], InstColor [37] and DeOldify [1]).

In order to embrace semantic information, some methods [12, 43] resort to generative adversarial networks (GANs) and utilize their rich representations as generative priors for colorization. However, due to the limited representation space of GAN prior, they fail to handle images with complex structures and semantics, leading to inappropriate colorization results or unpleasant artifacts (Fig. 1 Wu *et al.* [43] and BigColor [12]).

With the tremendous success in natural language pro-

cessing (NLP), Transformer [39] has been extended to many computer vision tasks. Recently, some works [23,42,44] introduce the non-local attention mechanism of transformer to image colorization. Though achieving promising results, these methods either train several independent sub-nets, leading to accumulated error (Fig. 1 ColTran [23]), or rely on hand-crafted dataset-level empirical distribution priors, failing to tackle complex image contexts (Fig. 1 CT2 [42] and ColorFormer [44]).

In this paper, we propose an end-to-end colorization network, namely DDColor, targeting at achieving semantically reasonable and visually vivid colorization. Our approach adopt an encoder-decoder structure, in which the encoder part extracts the features of the image and the decoder part restores the spatial resolution of the image. In particular, the decoder part is composed of two decoders, *i.e.*, a multi-scale image decoder and a transformer-based color decoder. The image decoder produces multi-scale visual features that are used by the color decoder to perform a set of adaptive color queries to learn semantic-aware color embedding. These two decoders incorporate to construct the final outputs. Over and above this, to improve the color richness of generated results, we present a new colorfulness loss.

We validate the performance of our model on three public benchmarks (ImageNet [35], COCO-Stuff [4], and ADE20k [51]) and conduct experiments to demonstrate the advantages of our framework. The visualization results and evaluation metrics show that our work achieves significant improvements to previous state-of-the-art methods in terms of semantic consistency, color richness, etc.

Our key contributions are:

- We develop a novel end-to-end network with dual decoders, namely DDColor, for automatic image colorization. A simple but effective colorfulness loss is introduced to obtain more vivid results.
- An image decoder and a color decoder are designed to produce multi-scale visual features and learn adaptive color queries from the visual features of large-scale data, respectively, contributing to natural and semantic consistent colorization.
- Comprehensive experiments demonstrate that our method achieves state-of-the-art performance in comparison with baselines.

2. Related Work

Reference-based colorization. Early attempts on image colorization rely on external references to guide the colorization process, such as additional user graffiti [24,31,34,46], user-specified reference images [13,21,41] and color statistics retrieved from the Internet [9,26]. The performance of these methods largely depends on the quality of the reference image. However, it is not easy to obtain a qualified reference image [9]. Recent works [17,45] use

deep neural networks (DNNs) to improve the spatial correspondence between grayscale images and reference images. Despite accomplishing a great success, it is still too complex and time-consuming for users.

Automatic colorization. The emergence of large-scale datasets and the development of DNNs make it possible to colorize grayscale images in a data-driven manner. Cheng *et al.* [8] propose the first DNN-based image colorization method. Zhang *et al.* [47] learn the color distribution of each pixel and train the network with a rebalanced multinomial cross-entropy, allowing rare colors to appear. MDN [10] uses a variational autoencoder (VAE) to get diverse colorized results. InstColor [37] believes that a clear figure-ground separation helps to improve performance of colorization, thus adopts a detection model to provide the detection box as prior. Later works [48,49] extend to take segmentation mask as pixel-level object semantics to guide colorization. Recently, some works [12,43] attempt to restore vivid color by taking advantage of the rich and diverse color priors of pre-trained GANs. They convert the grayscale image into a latent code by minimizing the structural difference between the input image and the color image generated from the latent space.

Vision transformer for colorization. Since successfully introduced Transformer [39] to vision recognition, Vision Transformer (ViT) [11] has developed rapidly in many downstream vision tasks including object detection [6,52] and segmentation [7,50]. In colorization, ColTran [23] uses a transformer to build a probability model, and samples color from the learning distribution to conditionally generate a low-resolution coarse colorization of the grayscale image, and then upsample it into a high-resolution image of fine color. CT2 [42] considers colorization as a classification task. It feeds color tokens and image patch tokens together into a ViT-based network, which includes a luminance-selecting module with pre-calculated probability distribution of dataset, to guide image colorization. ColorFormer [44] proposes a transformer-based network with hybrid self-attention. The image features are refined using a memory network with pre-built semantic-level color priors.

3. Method

3.1. Overview

Given a grayscale input image $x_L \in \mathbb{R}^{H \times W \times 1}$, our colorization network predicts the two missing color channels $\hat{y}_{AB} \in \mathbb{R}^{H \times W \times 2}$, where the L , AB channels represent the luminance and chrominance in CIELAB color space, respectively. The network is an encoder-decoder framework, as illustrated in Fig. 2. First, we leverage a backbone network as an image encoder to extract rich semantic information from grayscale images. Then, we use a image decoder to restore the spatial resolution of image fea-

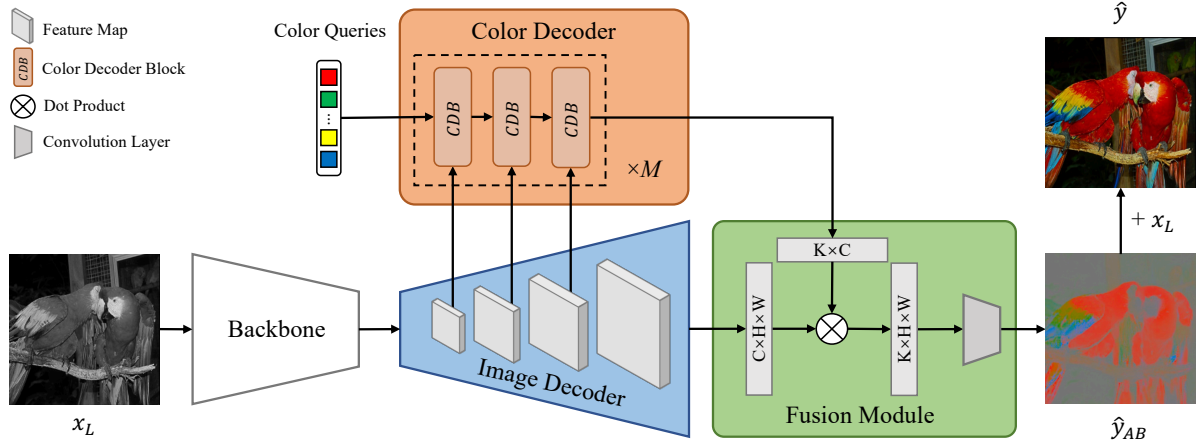


Figure 2. **Method overview.** Given a grayscale image x_L , our model first extract its visual features with a backbone network. The exacted features are feed to an image decoder to restore the spatial structure of the image. Meanwhile, a color decoder is introduced to assist color restoration via adaptive color queries. It is worth mentioning that the color decoder makes use of image features of different scales produced by the image decoder. A fusion module then merge the image and color features produced by the two decoders to yield a vivid and semantic-aware color output \hat{y}_{AB} . The final colorization result \hat{y} is obtained by concatenating \hat{y}_{AB} and x_L on the channel dimension.

tures through a plurality of stacked upsampling layers, each of which has a shortcut connection with the corresponding stage of the encoder. Meanwhile, we adopt a color decoder to obtain semantic-aware color embedding by leveraging adaptive color query operation on image features of different scales. Finally, with the image and color features produced by the above two decoders, we fuse them with a fusion module to output the color result. In the following, we elaborate on the detailed designs of these modules as well as the losses we used for colorization.

3.2. Backbone

Backbone network aims to extract image semantic embedding, which plays a key role in image colorization. In this work, we use ConvNeXt [28], which is the cutting-edge model for image classification. Taken $x_L \in \mathbb{R}^{H \times W \times 1}$ as input, the backbone network outputs 4 intermediate feature maps with resolutions of $\frac{H}{4} \times \frac{W}{4}$, $\frac{H}{8} \times \frac{W}{8}$, $\frac{H}{16} \times \frac{W}{16}$ and $\frac{H}{32} \times \frac{W}{32}$. The first three features are fed to image decoder through shortcut connections, while the last map is used as input of the image decoder. For the structure of backbone network, there are several options, such as Swin-Transformer [27], ResNet [16], etc., as long as the network produces a hierarchical representation.

3.3. Dual Decoders

The decoder part of DDColor is designed to introduce the color information into the grayscale image features, which is the essential component of the whole framework. As shown in the Fig. 2, the decoder part is composed of two parts, an image decoder and a color decoder. Next, we describe the details of these two modules.

3.3.1 Image Decoder

The image decoder consists of four stages that gradually expand the image resolution. Each stage includes an upsampling layer and a shortcut layer. Specifically, other than the deconvolution [33] or interpolation [29] used by previous methods, we use PixelShuffle [36] as the upsampling layer, which rearranges low-resolution feature maps with the shape of $(\frac{h}{p}, \frac{w}{p}, cp^2)$ into high-resolution ones with the shape of (h, w, c) . The shortcut layer uses a convolution to integrate the feature from the corresponding stages of the encoder through shortcut connections. Thanks to the step-by-step upsampling process, our method can capture a complete feature pyramid beyond the capability of some previous transformer-based methods [23, 42]. These multi-scale features are further used as the input of the color decoder to guide the optimization of the color queries. The final output of the image decoder is the image embedding $E_i \in \mathbb{R}^{C \times H \times W}$, which has the same spatial resolution as the input image.

3.3.2 Color Decoder

Most existing colorization methods require additional priors to produce vivid results. For example, some methods [12, 43] use GAN prior, while others use pre-built semantic-color pairs [44] or empirical distribution statistics of training sets [42]. However, these methods merely perform well on specific datasets and require much human effort to hand-craft priors for different scenarios. To alleviate the reliance on priors, we propose a new color decoder.

The color decoder consists of a stack of blocks, each

of them receives visual features and color queries as input. The color decoder block (CDB) is designed based on the modified transformer decoder, as shown in Fig. 3. The goal of the color decoder is to learn a set of adaptive color embedding based on visual semantic information. For this reason, we create learnable color embedding memories to store the sequence of color representations: $Z_0 = [Z_0^1, Z_0^2, \dots, Z_0^K] \in \mathbb{R}^{K \times C}$. All of them are initialized to zero in the training phase. These color embeddings are used as color queries in the first CDB.

We first establish the correlation between semantic representation and color embedding through the cross-attention layer:

$$Z_l' = \text{softmax}(Q_l K_l^T) V_l + Z_{l-1}, \quad (1)$$

where l is the layer index, $Z_l \in \mathbb{R}^{N \times C}$ refers to N C -dimensional color embeddings at the l^{th} layer. $Q_l = f_Q(Z_{l-1}) \in \mathbb{R}^{N \times C}$, and $K_l, V_l \in \mathbb{R}^{H_l \times W_l \times C}$ are the image features under transformation $f_K(\cdot)$ and $f_V(\cdot)$, in which H_l and W_l are the spatial resolution of image features. f_Q, f_K and f_V are linear transformations.

With the above cross-attention operation, the representation of color embedding is augmented by the image features. Standard transformer layers are then adopted to transform the color embedding as follows:

$$Z_l'' = \text{MSA}(\text{LN}(Z_l')) + Z_l', \quad (2)$$

$$Z_l''' = \text{MLP}(\text{LN}(Z_l'')) + Z_l'', \quad (3)$$

$$Z_l = \text{LN}(Z_l'''), \quad (4)$$

where $\text{MSA}(\cdot)$ indicates the multi-head self-attention [39], $\text{MLP}(\cdot)$ denotes the feed forward network, $\text{LN}(\cdot)$ is the layer normalization [3]. It is worth mentioning that cross-attention is operated before self-attention in the proposed CDB. This is because color queries are zero-initialized and are semantically independent before entering the first self-attention layer.

Extending to multi-scale. Multi-scale features have been widely used in many computer vision tasks such as object detection [25] and image segmentation [15]. These features can also be used to boost the performance of image colorization (see the ablation studies in Sec. 4.3). In order to balance computational complexity and representation capacity, we select image features of three different scales.

Specifically, the intermediate visual features generated by the image decoder with the downsample rate of 1/16, 1/8, and 1/4 are used in the color decoder. We group blocks with 3 CDB per group. In each group, the multi-scale features are fed to CDBs in a sequence. We repeated the group for M times in a round-robin fashion. In total, the color decoder consists of $3M$ CDBs. We formulate the color decoder as follows:

$$E_c = \text{ColorDecoder}(Z_0, \mathcal{F}_1, \mathcal{F}_2, \mathcal{F}_3), \quad (5)$$

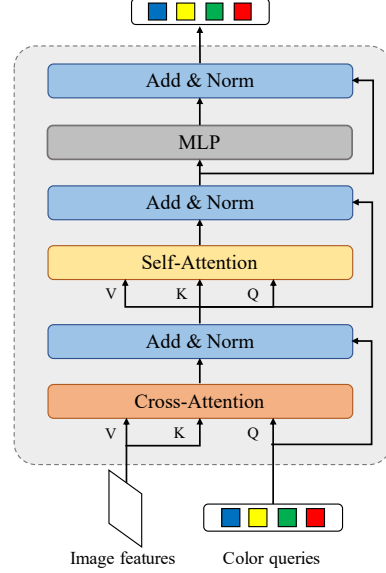


Figure 3. **Color Decoder Block.** The color decoder block receives image features and learnable color queries as inputs. It establishes the correlation between semantic and color representation by performing cross-attention, self-attention and feed forward operations, resulting in the color embedding optimized by visual features.

where $\mathcal{F}_1, \mathcal{F}_2$ and \mathcal{F}_3 are visual features at three different scales. In the color decoder, multi-scale features are used to model the relationship between color embedding and visual embeddings, making color embedding $E_c \in \mathbb{R}^{K \times C}$ more sensitive to semantic information.

3.4. Fusion Module

The fusion module is a lightweight module, which aggregates the outputs from the image decoder and the color decoder, and finally generates a color image. As presented in Fig. 2, the inputs of the fusion module are the per-pixel image embedding $E_i \in \mathbb{R}^{C \times H \times W}$ from the image decoder, where C is the embedding dimension, and semantic-aware color embedding $E_c \in \mathbb{R}^{K \times C}$ from the color decoder, where K is the number of color queries. The fusion module fuses these two embeddings to form an aggregate feature $\hat{\mathcal{F}} \in \mathbb{R}^{K \times H \times W}$ using a simple dot product, and then adopts a 1×1 convolution layer to get the final output $\hat{y}_{AB} \in \mathbb{R}^{2 \times H \times W}$, which represents the AB color channel:

$$\hat{\mathcal{F}} = E_c \cdot E_i, \quad (6)$$

$$\hat{y}_{AB} = \text{Conv}(\hat{\mathcal{F}}). \quad (7)$$

Finally, the colorization result \hat{y} is obtained by concatenating the predicted output \hat{y}_{AB} with the input grayscale image x_L .

Method	ImageNet (val5k)				ImageNet (val50k)				COCO-Stuff				ADE20K*			
	FID↓	CF↑	ΔCF↓	PSNR↑	FID↓	CF↑	ΔCF↓	PSNR↑	FID↓	CF↑	ΔCF↓	PSNR↑	FID↓	CF↑	ΔCF↓	PSNR↑
CIC [47]	8.72	31.60	6.61	22.64	19.17	43.92	4.83	20.86	27.88	33.84	4.40	22.73	15.31	31.92	3.12	23.14
InstColor [37]	8.06	24.87	13.34	23.28	7.36	27.05	12.04	22.91	13.09	27.45	10.79	23.38	15.44	23.54	11.50	24.27
DeOldify [1]	6.59	21.29	16.92	24.11	3.87	22.83	16.26	22.97	13.86	24.99	13.25	24.19	12.41	17.98	17.06	24.40
Wu <i>et al.</i> [43]	5.95	32.98	5.23	21.68	3.62	35.13	3.96	21.81	-	-	-	-	13.27	27.57	7.47	22.03
ColTran [23]	6.44	34.50	3.71	20.95	6.14	35.50	3.59	22.30	14.94	36.27	1.97	21.72	12.03	34.58	0.46	21.86
CT2 [42]	5.51	38.48	0.27	23.50	4.95	39.96	0.87	22.93	-	-	-	-	11.42	35.95	0.91	23.90
BigColor [12]	5.36	39.74	1.53	21.24	1.24	40.01	0.92	21.24	-	-	-	-	11.23	35.85	0.81	21.33
ColorFormer [44]	4.91	38.00	0.21	23.10	1.71	39.76	0.67	23.00	8.68	36.34	1.90	23.91	8.83	32.27	2.77	23.97
DDColor (Ours)	3.92	38.26	0.05	23.85	0.96	38.65	0.44	23.74	5.18	38.48	0.24	22.85	8.21	34.80	0.24	24.13

Table 1. **Quantitative comparison of different methods on benchmark datasets.** ↑ (↓) indicates higher (lower) is better. - means the results are unavailable. Particularly, the results on ADE20K dataset are reported by running their official codes.

3.5. Objectives

During the training phase, the following four losses are adopted:

Colorfulness loss. Referring to the colorfulness score [14], we introduce a new colorfulness loss \mathcal{L}_{col} in order to produce more colorful and visually pleasing images. It formulates as follow:

$$\mathcal{L}_{col} = 1 - [\sigma_{rgyb}(\hat{y}) + 0.3 \cdot \mu_{rgyb}(\hat{y})]/100, \quad (8)$$

where $\sigma_{rgyb}(\cdot)$ and $\mu_{rgyb}(\cdot)$ denote the standard deviation and the mean value of the pixel cloud in the color plane as described in [14], respectively.

Pixel loss. The pixel loss \mathcal{L}_{pix} is the L1 distance between the colorized image \hat{y} and the ground truth color image y , which helps the generator to output colors similar to the real image through pixel-level supervision.

Perceptual loss. In order to make the predicted image more semantically reasonable, we use a perceptual loss \mathcal{L}_{per} to minimize the semantic difference between the generated image \hat{y} and the real image y .

Adversarial loss. A PatchGAN [22] discriminator is added to tell apart predicted results and real images, pushing the generator to generate indistinguishable images. Let \mathcal{L}_{adv} denote the adversarial loss.

The full objective for the generator is formed as follow:

$$\mathcal{L}_\theta = \lambda_{pix}\mathcal{L}_{pix} + \lambda_{per}\mathcal{L}_{per} + \lambda_{adv}\mathcal{L}_{adv} + \lambda_{col}\mathcal{L}_{col}, \quad (9)$$

where λ_{pix} , λ_{per} , λ_{adv} and λ_{col} are balancing weights of different terms.

4. Experiments

4.1. Experimental Setting

Datasets. We conduct experiments on three datasets.

ImageNet [35] has been widely used by most existing colorization methods. It consists of 1.3M (50,000) images

for training (testing). It is worthy to note that some works [2, 23, 42] only use the first 5,000 images for validation.

COCO-Stuff [4] contains a wide variety of natural images. We test on the 5,000 images of the original validation set without fine-tuning.

ADE20K [51] is composed of scene-centric images with large diversity. We test on the 2,000 images of validation set without fine-tuning.

Evaluation metrics. Following the experimental protocol of existing colorization methods, we mainly use Fréchet inception distance (FID) [18] and colorfulness score (CF) [14] to evaluate the performance of our method, where FID measures the distribution similarity between generated images and ground truth images and CF reflects the vividness of generated images. We also provide Peak Signal-to-Noise Ratio (PSNR) [19] for reference, although it is a widely held view that the pixel-level metrics may not well reflect the actual colorization performance [5, 17, 32, 37, 40, 43, 44, 48].

Implementation details. We train our network with AdamW [30] optimizer and set $\beta_1 = 0.9$, $\beta_2 = 0.99$, weight decay = 0.01. The learning rate is initialized to $1e^{-4}$. For the loss terms, we set $\lambda_{pix} = 0.1$, $\lambda_{per} = 5.0$, $\lambda_{adv} = 1.0$ and $\lambda_{col} = 0.5$. We use ConvNeXt-L as the backbone network. For the image decoder, the feature dimensions after four upsampling stages are 512, 512, 256, and 256, respectively. For the color decoder, we set $M = 3$, $K = 100$. The whole network is trained in an end-to-end self-supervised fashion for 400,000 iterations with batch size of 16 and the learning rate is decayed by 0.5 at 80,000 iterations and every 40,000 iterations thereafter. We adopt color augmentation [12] to real color images during training. The training images are resized into 256×256 resolution. All experiments are conducted on 4 Tesla V100 GPUs.

4.2. Comparison with State-of-the-Art Methods

Quantitative comparison. We benchmark our method against previous methods on three datasets and report quantitative results in Tab. 1. For all previous methods, we con-

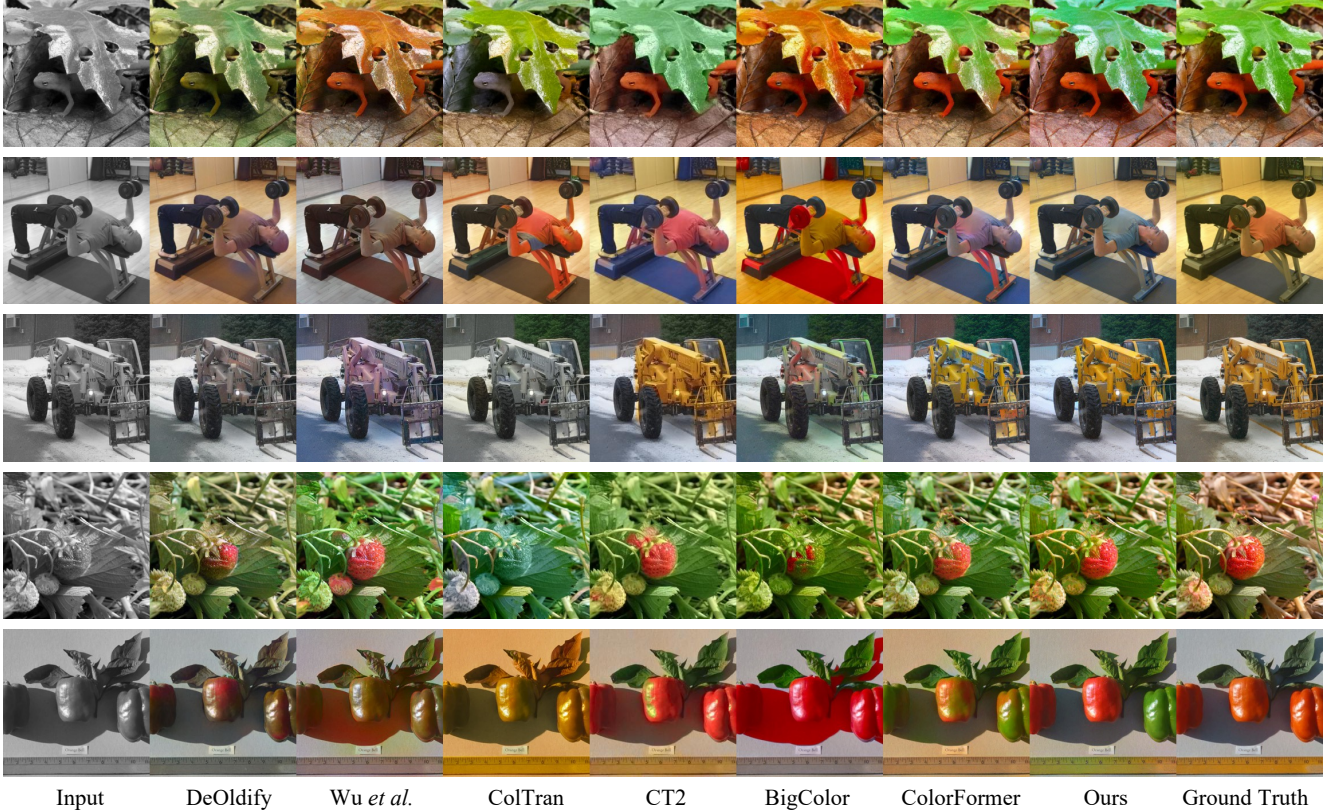


Figure 4. **Visual comparison of competing methods on automatic image colorization.** All the images are from the ImageNet validation set. One can see that our method generates more natural and vivid colors than SOTAs.

ducted tests using their official codes and weights from the authors. On the ImageNet dataset, our method achieves the lowest FID, indicating that our method can produce high-quality and high-fidelity colorization results. Our method also achieves the lowest FID on the COCO-Stuff and ADE20K datasets, which demonstrates the good generalization of our method. The colorfulness score can reflect the vividness of the image. It can be seen that some methods [12, 42, 47] report higher scores than ours. However, high colorfulness score does not always mean good visual quality (see the 6th column of Fig. 4). Therefore, we further calculate ΔCF to report the colorfulness score difference between the generated image and the ground truth image. Our method achieves the lowest ΔCF on all datasets, indicating that our method generates more natural and realistic colorization results.

Qualitative evaluation. We visualize the image colorization results in Fig. 4. Note that ground truth images are for reference only, and the evaluation criteria should not be color similarity due to the multi-modal uncertainty of the problem. It is observable that our results are more natural and vivid compared with other competitors. As we can see, DeOldify [1] tends to produce dull and unsaturated images.

ColTran [23] accumulates errors because the three subnets are trained independently, leading to noticeable unnatural colorization results, such as lizards (row 1) and vegetables (row 5). Wu *et al.* [43] and BigColor [12], both based on the GAN prior, produce unpleasant red artifacts on shadows (row 2 and 5) and vehicles (row 3). CT2 [42] and ColFormer [44] occasionally produce incorrect colorization results especially in scenarios with complex image semantics (the person in row 2). Instead, our approach generates semantically reasonable and visually pleasing colorization results for complex scenes such as lizards and leaves (row 1) or men in the gym (row 2), and successfully maintains the consistent tone and captures the details of salient object in a picture such as vehicles (row 3) and strawberries (row 4). It is also capable of generating diverse colors such as the vegetables (row 5). More visual comparison results on different datasets can be found in the supplementary material.

User study. We conducted a user study to investigate the subjective preference of human observers for each colorization method. Specifically, we compare our method with DeOldify [1], BigColor [12], CT2 [42] and ColorFormer [44]. We randomly select 50 input images from the ImageNet validation set together with the coloring results displayed to 20

ColorDec.	\mathcal{L}_{col}	FID↓	CF↑	ΔCF_{\downarrow}
×	×	6.04	33.07	5.14
×	✓	5.93	36.14	2.07
✓	×	4.01	35.69	2.52
✓	✓	3.92	38.26	0.05

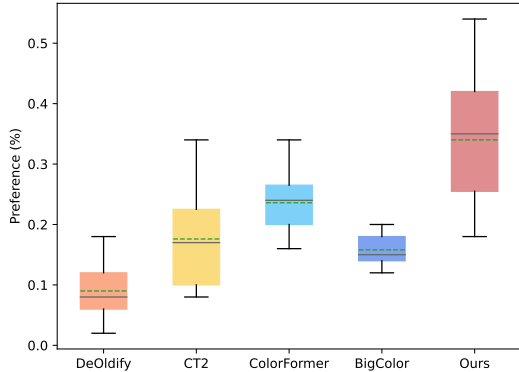
(a) Color Decoder and Colorfulness Loss.

Feature Scales	FID↓	CF↑	ΔCF_{\downarrow}
single scale (1/16)	5.09	37.22	0.99
single scale (1/8)	4.49	37.58	0.63
single scale (1/4)	4.44	37.74	0.47
multi-scale (3 scales)	3.92	38.26	0.05

(b) Different Feature Scales.

Decoder Architecture	FID↓	CF↑	ΔCF_{\downarrow}
self-attn. + self-attn.	8.74	51.98	13.77
cross-attn. + cross-attn.	4.55	39.93	1.72
self-attn. + cross-attn.	3.98	37.70	0.51
cross-attn. + self-attn.	3.92	38.26	0.05

(c) Color Decoder Architecture.

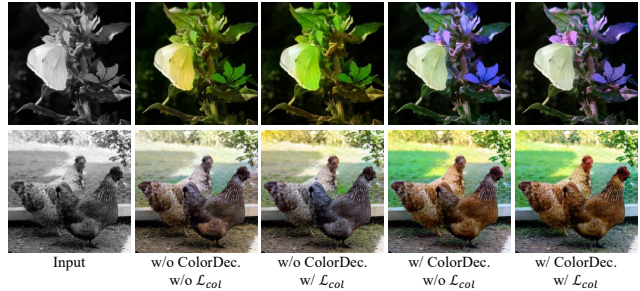
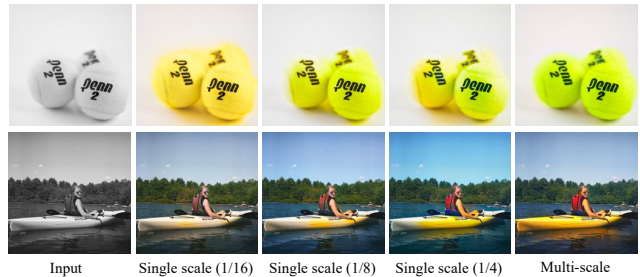
Table 2. **Ablation studies.** All the experiment are conducted using ImageNet (val5k) validation set.Figure 5. **Boxplot of user study.** The dashed green line and the solid gray line inside the bars are the mean and the median preference percentage, respectively.

subjects. Subjects select the best colorized image from the randomly shuffle results of different methods. As shown in Fig. 5, our method is preferred by a wider range of users than the state-of-the-art methods.

4.3. Ablation Study

Here, we perform an ablation study to validate the effects of several important design options in our model. In all ablation study experiments, we use the same first 5,000 images of the ImageNet validation dataset for testing. Besides the ablation design choices, we use the same training configuration unless explicitly stated. More ablations and visual results can be referred to supplementary material.

Color decoder and colorfulness loss. We construct a variant of our model that excludes color decoder, *i.e.*, the entire network structure contains only the backbone and the image decoder. We then train both our full model and its variant twice, with and without colorfulness loss. As shown in Tab. 2a and Fig. 6, the proposed color decoder plays an important role in the final colorization result because of the adaptive color queries learned from diverse semantic features. Compared with baselines, the method with color decoder can achieve more natural and semantically reasonable colorization on diverse objects (such as butterflies and flowers in row 1, roosters and lawns in row 2). It can also be seen

Figure 6. **Visual results of ablation on color decoder and colorfulness loss.**Figure 7. **Visual results of ablation on different feature scales.**

that the introducing colorfulness loss helps improve the colorfulness of the final result.

Multi-scale vs. single scale. To evaluate the effect of multi-scale features, we conduct 3 variants that use single scale features at different scales. The results in Fig. 7 show that the 3 variants tend to produce suboptimal colorization results, inaccurate colorization results at the edges of objects (such as tennis in row 1), and semantically inconsistent colors for objects with different scales (such as people and kayak in row 2). With multi-scale features, our full model captures more semantic structure information and produces more natural and accurate colorization results.

Color decoder architecture. The color decoder architecture is designed for the purpose of using visual semantic information for learning color embeddings. We conduct ablation studies to validate the importance of each key component by modifying their arrangement. As shown in Tab. 2c, we can see that both cross-attention layer and self-attention layer are essential for robust image colorization. This is

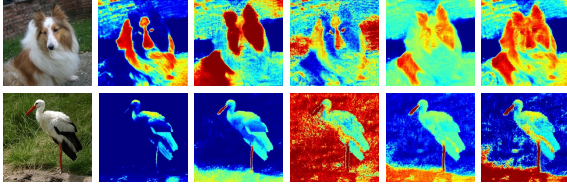


Figure 8. **Visualization of learned color queries.** The left column is the colorized image by our method, and columns on the right are the visualization of color queries. Red (blue) represents high (low) activation values.

# of queries	FID↓	CF↑	Δ CF↓
20	4.02	37.86	0.35
50	3.96	38.00	0.21
100	3.92	38.26	0.05
200	3.96	37.71	0.50
500	3.93	37.88	0.33

Table 3. **Ablation on the number of color queries.** The model with 100 queries performs best on ImageNet dataset.

because using merely the self-attention layer or the cross-attention layer lead to poor colorization results. Additionally, the sequence of self-attention and cross-attention layers also matters.

Number of color queries. We vary the number of color queries to evaluate its effect. As shown in Sec. 4.3, the performance reaches to the peak at 100 queries. Several previous approaches [42,47] consider colorization as a classification problem and quantify the AB color space into 313 categories. In our approach, the learned color queries are adequate to represent color embeddings in the color space with much fewer categories. Interestingly, even with only 20 queries, our method outperforms the previous classification-based methods [42,47] on FID.

4.4. Visualizing the Color Queries

We visualize the learned color queries to reveal how it works. See Fig. 8. Visualization results are obtained by sigmoiding the dot product of the single color query and the image feature map. It can be seen that different color queries have different high activation regions on the image feature map. Taken the first row as an example, the first color query attends on the forehead, nose and body of the dog, which captures the white color embedding. The second and third color queries focus on the fur of the dog and grass background regions, which capture brown and green color embeddings, respectively.

4.5. Visual Results on Real-world Black-and-white Photos

We collect some real historical black-and-white photos to demonstrate the capability of our method in real-world



Figure 9. **Colorizing legacy photographs.** From top to bottom are respectively the input, the manually colorized results by human experts and our results.



Figure 10. **Failure Cases.** Our method may still produce visual artifacts when coloring transparent/translucent objects with different colors.

scenarios. Fig. 9 shows the results of our method, as well as the manual colorization results by human experts¹², indicating the practicability of our approach.

4.6. Limitation

As shown in Fig. 10, there are still failure cases when dealing with out-of-distribution images, such as those with transparent/translucent objects. Further improvement may require extra semantic supervision to help the network better understand such complex scenarios.

5. Conclusion

In this work, we propose an end-to-end method, namely DDColor, for image colorization. The key contribution of DDColor lies in the design of two decoders, where the color decoder aims to learn semantic-aware color embedding via adaptive color queries, and the image decoder produces multi-scale visual features to help optimize the aforementioned color queries. Comparison with previous methods shows that our approach both achieves state-of-the-art performance and generates realistic and semantic consistent colorization.

¹reddit.com/r/ArchitecturePorn

²justsomething.co/34-incredible-colored-photos

References

- [1] Jason Antic. jantic/deoldify: A deep learning based project for colorizing and restoring old images (and video!). <https://github.com/jantic/DeOldify>, 2019. **1, 5, 6, 11**
- [2] Lynton Ardizzone, Carsten Lüth, Jakob Kruse, Carsten Rother, and Ullrich Köthe. Guided image generation with conditional invertible neural networks. *arXiv preprint arXiv:1907.02392*, 2019. **5**
- [3] Jimmy Lei Ba, Jamie Ryan Kiros, and Geoffrey E Hinton. Layer normalization. *arXiv preprint arXiv:1607.06450*, 2016. **4**
- [4] Holger Caesar, Jasper Uijlings, and Vittorio Ferrari. Cocomstuff: Thing and stuff classes in context. In *Proceedings of the IEEE conference on computer vision and pattern recognition*, pages 1209–1218, 2018. **2, 5, 11**
- [5] Yun Cao, Zhiming Zhou, Weinan Zhang, and Yong Yu. Unsupervised diverse colorization via generative adversarial networks. In *Joint European conference on machine learning and knowledge discovery in databases*, pages 151–166. Springer, 2017. **5**
- [6] Nicolas Carion, Francisco Massa, Gabriel Synnaeve, Nicolas Usunier, Alexander Kirillov, and Sergey Zagoruyko. End-to-end object detection with transformers. In *European conference on computer vision*, pages 213–229. Springer, 2020. **2**
- [7] Bowen Cheng, Alex Schwing, and Alexander Kirillov. Per-pixel classification is not all you need for semantic segmentation. *Advances in Neural Information Processing Systems*, 34:17864–17875, 2021. **2**
- [8] Zezhou Cheng, Qingxiong Yang, and Bin Sheng. Deep colorization. In *Proceedings of the IEEE international conference on computer vision*, pages 415–423, 2015. **1, 2**
- [9] Alex Yong-Sang Chia, Shaojie Zhuo, Raj Kumar Gupta, Yu-Wing Tai, Siu-Yeung Cho, Ping Tan, and Stephen Lin. Semantic colorization with internet images. *ACM Transactions on Graphics (TOG)*, 30(6):1–8, 2011. **1, 2**
- [10] Aditya Deshpande, Jiajun Lu, Mao-Chuang Yeh, Min Jin Chong, and David Forsyth. Learning diverse image colorization. In *Proceedings of the IEEE Conference on Computer Vision and Pattern Recognition*, pages 6837–6845, 2017. **1, 2**
- [11] Alexey Dosovitskiy, Lucas Beyer, Alexander Kolesnikov, Dirk Weissenborn, Xiaohua Zhai, Thomas Unterthiner, Mostafa Dehghani, Matthias Minderer, Georg Heigold, Sylvain Gelly, et al. An image is worth 16x16 words: Transformers for image recognition at scale. *arXiv preprint arXiv:2010.11929*, 2020. **2**
- [12] Kim Geonung, Kang Kyoungkook, Kim Seongtae, Lee Hwayoon, Kim Sehoon, Kim Jonghyun, Baek Seung-Hwan, and Cho Sunghyun. Bigcolor: Colorization using a generative color prior for natural images. In *European Conference on Computer Vision (ECCV)*, 2022. **1, 2, 3, 5, 6, 11**
- [13] Raj Kumar Gupta, Alex Yong-Sang Chia, Deepu Rajan, Ee Sin Ng, and Huang Zhiyong. Image colorization using similar images. In *Proceedings of the 20th ACM international conference on Multimedia*, pages 369–378, 2012. **1, 2**
- [14] David Hasler and Sabine E Suesstrunk. Measuring colorfulness in natural images. In *Human vision and electronic imaging VIII*, volume 5007, pages 87–95. SPIE, 2003. **5**
- [15] Kaiming He, Georgia Gkioxari, Piotr Dollár, and Ross Girshick. Mask r-cnn. In *Proceedings of the IEEE international conference on computer vision*, pages 2961–2969, 2017. **4**
- [16] Kaiming He, Xiangyu Zhang, Shaoqing Ren, and Jian Sun. Deep residual learning for image recognition. In *Proceedings of the IEEE conference on computer vision and pattern recognition*, pages 770–778, 2016. **3**
- [17] Mingming He, Dongdong Chen, Jing Liao, Pedro V Sander, and Lu Yuan. Deep exemplar-based colorization. *ACM Transactions on Graphics (TOG)*, 37(4):1–16, 2018. **2, 5**
- [18] Martin Heusel, Hubert Ramsauer, Thomas Unterthiner, Bernhard Nessler, and Sepp Hochreiter. Gans trained by a two time-scale update rule converge to a local nash equilibrium. *Advances in neural information processing systems*, 30, 2017. **5**
- [19] Quan Huynh-Thu and Mohammed Ghanbari. Scope of validity of psnr in image/video quality assessment. *Electronics letters*, 44(13):800–801, 2008. **5**
- [20] Satoshi Iizuka and Edgar Simo-Serra. Deepremaster: temporal source-reference attention networks for comprehensive video enhancement. *ACM Transactions on Graphics (TOG)*, 38(6):1–13, 2019. **1**
- [21] Revital Ironi, Daniel Cohen-Or, and Dani Lischinski. Colorization by example. *Rendering techniques*, 29:201–210, 2005. **1, 2**
- [22] Phillip Isola, Jun-Yan Zhu, Tinghui Zhou, and Alexei A Efros. Image-to-image translation with conditional adversarial networks. In *Proceedings of the IEEE conference on computer vision and pattern recognition*, pages 1125–1134, 2017. **5**
- [23] Manoj Kumar, Dirk Weissenborn, and Nal Kalchbrenner. Colorization transformer. In *International Conference on Learning Representations*, 2021. **2, 3, 5, 6, 11**
- [24] Anat Levin, Dani Lischinski, and Yair Weiss. Colorization using optimization. In *ACM SIGGRAPH 2004 Papers*, pages 689–694. 2004. **1, 2**
- [25] Wei Liu, Dragomir Anguelov, Dumitru Erhan, Christian Szegedy, Scott Reed, Cheng-Yang Fu, and Alexander C Berg. Ssd: Single shot multibox detector. In *European conference on computer vision*, pages 21–37. Springer, 2016. **4**
- [26] Xiaopei Liu, Liang Wan, Yingge Qu, Tien-Tsin Wong, Stephen Lin, Chi-Sing Leung, and Pheng-Ann Heng. Intrinsic colorization. In *ACM SIGGRAPH Asia 2008 papers*, pages 1–9. 2008. **1, 2**
- [27] Ze Liu, Yutong Lin, Yue Cao, Han Hu, Yixuan Wei, Zheng Zhang, Stephen Lin, and Baining Guo. Swin transformer: Hierarchical vision transformer using shifted windows. In *Proceedings of the IEEE/CVF International Conference on Computer Vision*, pages 10012–10022, 2021. **3**
- [28] Zhuang Liu, Hanzi Mao, Chao-Yuan Wu, Christoph Feichtenhofer, Trevor Darrell, and Saining Xie. A convnet for the 2020s. In *Proceedings of the IEEE/CVF Conference on Computer Vision and Pattern Recognition*, pages 11976–11986, 2022. **3, 11**

- [29] Jonathan Long, Evan Shelhamer, and Trevor Darrell. Fully convolutional networks for semantic segmentation. In *Proceedings of the IEEE conference on computer vision and pattern recognition*, pages 3431–3440, 2015. 3
- [30] Ilya Loshchilov and Frank Hutter. Decoupled weight decay regularization. *arXiv preprint arXiv:1711.05101*, 2017. 5
- [31] Qing Luan, Fang Wen, Daniel Cohen-Or, Lin Liang, Ying-Qing Xu, and Heung-Yeung Shum. Natural image colorization. In *Proceedings of the 18th Eurographics conference on Rendering Techniques*, pages 309–320, 2007. 1, 2
- [32] Safa Messaoud, David Forsyth, and Alexander G Schwing. Structural consistency and controllability for diverse colorization. In *Proceedings of the European Conference on Computer Vision (ECCV)*, pages 596–612, 2018. 5
- [33] Hyeonwoo Noh, Seunghoon Hong, and Bohyung Han. Learning deconvolution network for semantic segmentation. In *Proceedings of the IEEE international conference on computer vision*, pages 1520–1528, 2015. 3
- [34] Yingge Qu, Tien-Tsin Wong, and Pheng-Ann Heng. Manga colorization. *ACM Transactions on Graphics (TOG)*, 25(3):1214–1220, 2006. 1, 2
- [35] Olga Russakovsky, Jia Deng, Hao Su, Jonathan Krause, Sanjeev Satheesh, Sean Ma, Zhiheng Huang, Andrej Karpathy, Aditya Khosla, Michael Bernstein, et al. Imagenet large scale visual recognition challenge. *International journal of computer vision*, 115(3):211–252, 2015. 2, 5, 11
- [36] Wenzhe Shi, Jose Caballero, Ferenc Huszár, Johannes Totz, Andrew P Aitken, Rob Bishop, Daniel Rueckert, and Zehan Wang. Real-time single image and video super-resolution using an efficient sub-pixel convolutional neural network. In *Proceedings of the IEEE conference on computer vision and pattern recognition*, pages 1874–1883, 2016. 3
- [37] Jheng-Wei Su, Hung-Kuo Chu, and Jia-Bin Huang. Instance-aware image colorization. In *Proceedings of the IEEE/CVF Conference on Computer Vision and Pattern Recognition*, pages 7968–7977, 2020. 1, 2, 5
- [38] Sotirios A Tsaftaris, Francesca Casadio, Jean-Louis Andral, and Aggelos K Katsaggelos. A novel visualization tool for art history and conservation: Automated colorization of black and white archival photographs of works of art. *Studies in conservation*, 59(3):125–135, 2014. 1
- [39] Ashish Vaswani, Noam Shazeer, Niki Parmar, Jakob Uszkoreit, Llion Jones, Aidan N Gomez, Łukasz Kaiser, and Illia Polosukhin. Attention is all you need. *Advances in neural information processing systems*, 30, 2017. 2, 4
- [40] Patricia Vitoria, Lara Raad, and Coloma Ballester. Chromagan: Adversarial picture colorization with semantic class distribution. In *Proceedings of the IEEE/CVF Winter Conference on Applications of Computer Vision*, pages 2445–2454, 2020. 5
- [41] Tomihisa Welsh, Michael Ashikhmin, and Klaus Mueller. Transferring color to greyscale images. In *Proceedings of the 29th annual conference on Computer graphics and interactive techniques*, pages 277–280, 2002. 1, 2
- [42] Shuchen Weng, Jimeng Sun, Yu Li, Si Li, and Boxin Shi. Ct2: Colorization transformer via color tokens. In *European Conference on Computer Vision (ECCV)*, 2022. 2, 3, 5, 6, 8, 11
- [43] Yanze Wu, Xintao Wang, Yu Li, Honglun Zhang, Xun Zhao, and Ying Shan. Towards vivid and diverse image colorization with generative color prior. In *Proceedings of the IEEE/CVF International Conference on Computer Vision*, 2021. 1, 2, 3, 5, 6, 11
- [44] Ji Xiaozhong, Boyuan Jiang, Luo Donghao, Tao Guangpin, Chu Wenqing, Xie Zhifeng, Wang Chengjie, and Tai Ying. Colorformer: Image colorization via color memory assisted hybrid-attention transformer. In *European Conference on Computer Vision (ECCV)*, 2022. 2, 3, 5, 6, 11
- [45] Zhongyou Xu, Tingting Wang, Faming Fang, Yun Sheng, and Guixu Zhang. Stylization-based architecture for fast deep exemplar colorization. In *Proceedings of the IEEE/CVF Conference on Computer Vision and Pattern Recognition*, pages 9363–9372, 2020. 2
- [46] Liron Yatziv and Guillermo Sapiro. Fast image and video colorization using chrominance blending. *IEEE transactions on image processing*, 15(5):1120–1129, 2006. 1, 2
- [47] Richard Zhang, Phillip Isola, and Alexei A Efros. Colorful image colorization. In *European conference on computer vision*, pages 649–666. Springer, 2016. 1, 2, 5, 6, 8
- [48] Jiaojiao Zhao, Jungong Han, Ling Shao, and Cees GM Snoek. Pixelated semantic colorization. *International Journal of Computer Vision*, 128(4):818–834, 2020. 2, 5
- [49] Jiaojiao Zhao, Li Liu, Cees GM Snoek, Jungong Han, and Ling Shao. Pixel-level semantics guided image colorization. *arXiv preprint arXiv:1808.01597*, 2018. 2
- [50] Sixiao Zheng, Jiachen Lu, Hengshuang Zhao, Xiatian Zhu, Zekun Luo, Yabiao Wang, Yanwei Fu, Jianfeng Feng, Tao Xiang, Philip HS Torr, et al. Rethinking semantic segmentation from a sequence-to-sequence perspective with transformers. In *Proceedings of the IEEE/CVF conference on computer vision and pattern recognition*, pages 6881–6890, 2021. 2
- [51] Bolei Zhou, Hang Zhao, Xavier Puig, Sanja Fidler, Adela Barriuso, and Antonio Torralba. Scene parsing through ade20k dataset. In *Proceedings of the IEEE conference on computer vision and pattern recognition*, pages 633–641, 2017. 2, 5, 11
- [52] Xizhou Zhu, Weijie Su, Lewei Lu, Bin Li, Xiaogang Wang, and Jifeng Dai. Deformable detr: Deformable transformers for end-to-end object detection. *arXiv preprint arXiv:2010.04159*, 2020. 2

DDColor: Towards Photo-Realistic and Semantic-Aware Image Colorization via Dual Decoders

Appendix

In this supplementary document, we provide the following materials to complement the main manuscript:

- Detailed network architecture of DDColor;
- Additional qualitative results;
- Additional ablation study and visual results;
- Runtime analysis;
- More results on legacy black and white photos.

A. Detailed Network Architecture

We list the detailed architecture of DDColor with a ConvNeXt-T [28] backbone in Tab. 4. The resolution of the input image is 256×256 .

B. Additional Qualitative Results

Here, we show more qualitative comparisons with previous methods on ImageNet [35] validation in Fig. 11. As in the main paper, we compare our method with DeOldify [1], Wu *et al.* [43], ColTran [23], CT2 [42], BigColor [12] and ColorFormer [44]. The visual comparisons on COCO-Stuff [4] and ADE20K [51] are also presented in Fig. 12 and Fig. 13, respectively. It can be seen that our method achieves more natural and vivid results in diverse scenarios, and produces more semantically consistent colors for a variety of objects.

C. Additional Ablation Study and Visual Results

We build four variants of our model with different ConvNeXt [28] backbones, as detailed in Appendix C. As can be seen, the backbone plays a key role in image colorization. We choose ConvNeXt-L due to its superior performance.

More visual results on ablations of color decoder, colorfulness loss, and different visual feature scales are shown in Fig. 14 and Fig. 15.

D. Runtime Analysis

Our method colorizes grayscale images of resolution 256×256 at 25 FPS / 21 FPS using ConvNeXt-T / ConvNeXt-L as the backbone. The inference speed of our end-to-end method is $\times 96$ faster than the previous transformer-based method [23]. All tests are performed on a machine with an NVIDIA Tesla V100 32G GPU.

E. More Results on Legacy Black and White Photos

More colorization results on legacy black and white photos are shown in Fig. 16, demonstrating the generalization capability of our method.

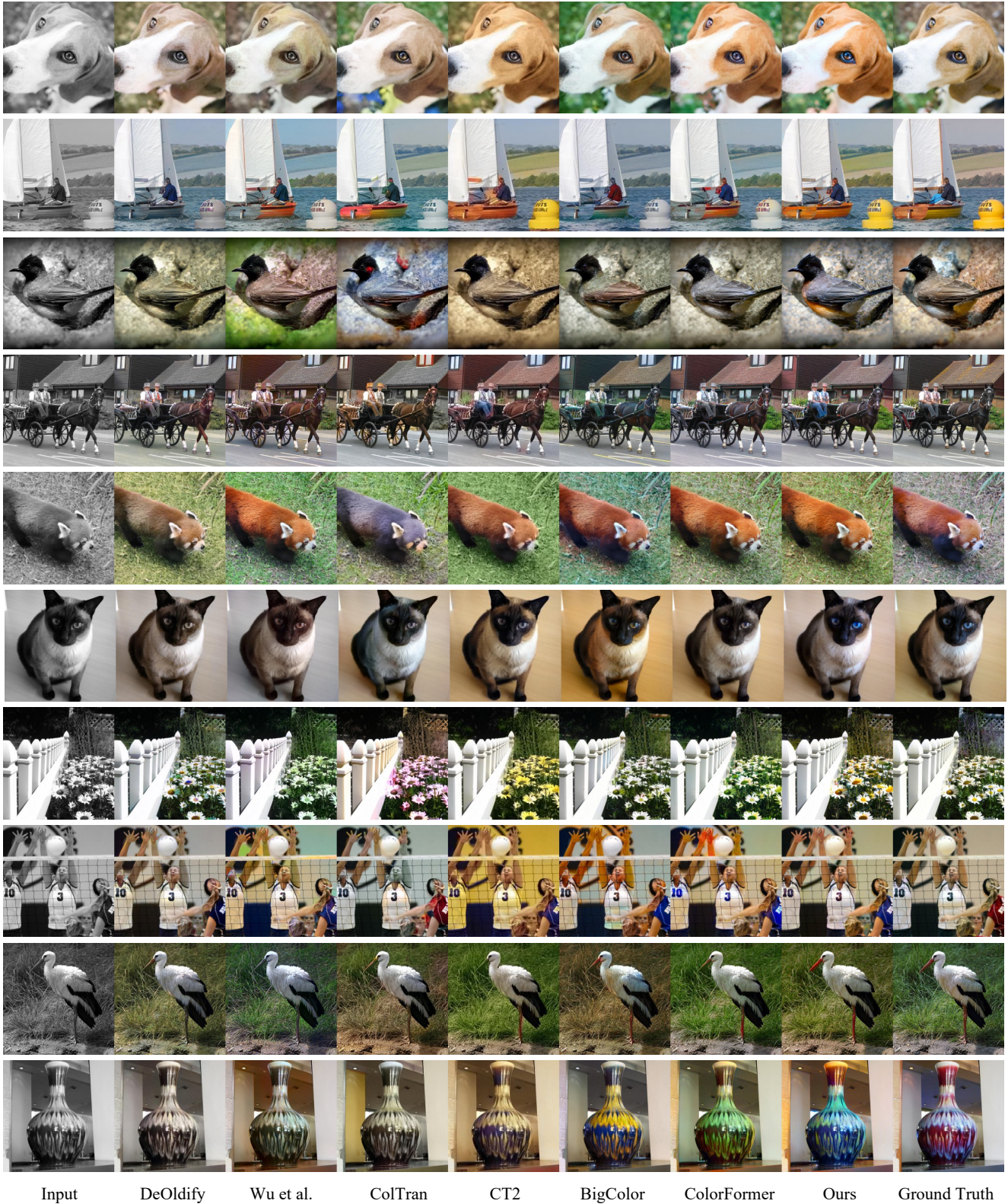


Figure 11. More qualitative comparisons with previous colorization methods on ImageNet.

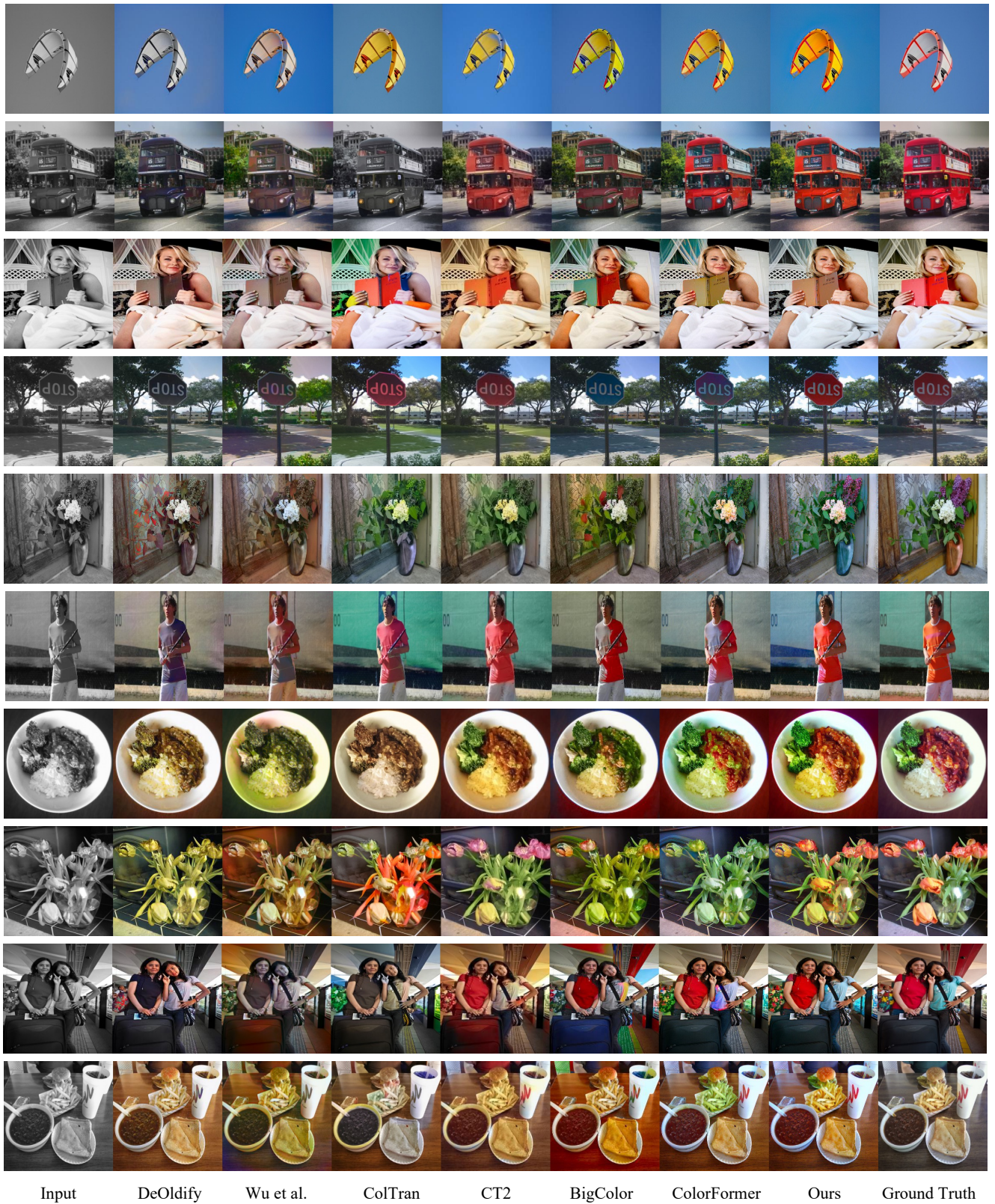


Figure 12. Qualitative comparisons with previous colorization methods on COCO-Stuff.



Figure 13. Qualitative comparisons with previous colorization methods on ADE20K.

	Output size	DDColor
Stage 1	$64 \times 64 \times 96$	Conv. 4×4 , 96, stride 4 Depthwise Conv. 7×7, 96 Conv. 1×1, 384 Conv. 1×1, 96 $\times 3$
Stage 2	$32 \times 32 \times 192$	Depthwise Conv. 7×7, 192 Conv. 1×1, 768 Conv. 1×1, 192 $\times 3$
Stage 3	$16 \times 16 \times 384$	Depthwise Conv. 7×7, 384 Conv. 1×1, 1536 Conv. 1×1, 384 $\times 9$
Stage 4	$8 \times 8 \times 768$	Depthwise Conv. 7×7, 768 Conv. 1×1, 3072 Conv. 1×1, 768 $\times 3$
Stage 5	$16 \times 16 \times 512$	PixelShuffle, scale 2 Concat feat. from Stage 3 Conv. 3×3 , 512
Stage 6	$32 \times 32 \times 512$	PixelShuffle, scale 2 Concat feat. from Stage 2 Conv. 3×3 , 512
Stage 7	$64 \times 64 \times 256$	PixelShuffle, scale 2 Concat feat. from Stage 1 Conv. 3×3 , 256
Stage 8	$256 \times 256 \times 256$	PixelShuffle, scale 4
Color Dec.	256×100	Conv. 1×1 , 256 feat. from Stage 5 Conv. 1×1 , 256 feat. from Stage 6 Conv. 1×1 , 256 feat. from Stage 7 Conv. 1×1, 256×3 Cross-attn. Self-attn. Conv. 1×1, 2048 Conv. 1×1, 256 $\times 9$
Stage 9	$256 \times 256 \times 100$	Dot Product feat. from Stage 8 & feat. from Color Dec.
Stage 10	$256 \times 256 \times 2$	Concat input Conv. 1×1 , 2

Table 4. Detailed architecture of DDColor.

Backbone	FID↓	CF↑	Δ CF↓	Params
ConvNeXt-T	4.39	37.63	0.58	55.0M
ConvNeXt-S	4.25	38.10	0.11	76.6M
ConvNeXt-B	4.06	38.15	0.06	116.2M
ConvNeXt-L	3.92	38.26	0.05	227.9M

Table 5. **Backbone variants.** We build four variants of our DDColor based on backbones of different sizes. The overall performance improves with the increase of the scale of the backbone network.



Figure 14. More visual results of ablation on color decoder and colorfulness loss.

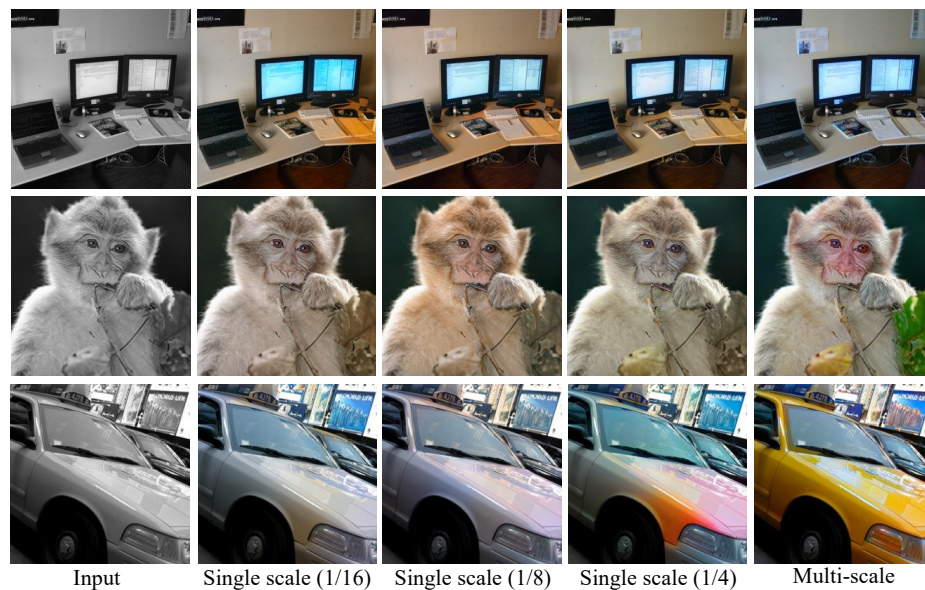
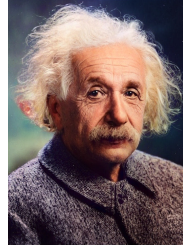
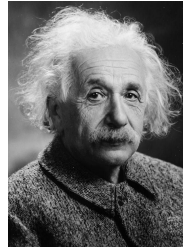


Figure 15. More visual results of ablation on different feature scales.



1931. "New York Riverfront."

1899. "Sailing ship Mary L. Cushing."

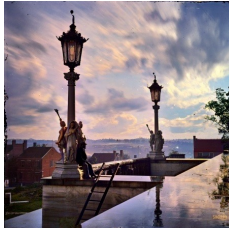
1947. "Albert Einstein."



1945. "Abandoned boy holding a stuffed toy animal."

circa 1894-1901. "Miss H.M. Craig."

1915. "Woodward Avenue and Campus Martius, Detroit, Michigan."



circa 1900-1915. "Broadway at the United States Hotel Saratoga Springs."

1946. "Louis Armstrong practicing in his dressing room."

1864. "View from the Capitol at Nashville, Tennessee."

Figure 16. More results on legacy black and white photos.